

## 2.6 PIEZOELECTRIC SENSORS

*Piezoelectric sensors* are used to measure physiological displacements and record heart sounds. Piezoelectric materials generate an electric potential when mechanically strained, and conversely an electric potential can cause physical deformation of the material. The principle of operation is that when an asymmetrical crystal lattice is distorted, a charge reorientation takes place, causing a relative displacement of negative and positive charges. The displaced internal charges induce surface charges of opposite polarity on opposite sides of the crystal. Surface charge can be determined by measuring the difference in voltage between electrodes attached to the surfaces.

Initially, we assume infinite leakage resistance. Then, the total induced charge  $q$  is directly proportional to the applied force  $f$ .

$$q = kf \quad (2.13)$$

where  $k$  is the piezoelectric constant, C/N. The change in voltage can be found by assuming that the system acts like a parallel-plate capacitor where the voltage  $v$  across the capacitor is charge  $q$  divided by capacitance  $C$ . Then, by substitution of (2.8), we get

$$v = \frac{kf}{C} = \frac{kfx}{\epsilon_0 \epsilon_r A} \quad (2.14)$$

Tables of piezoelectric constants are given in the literature (Lion, 1959; and Cobbold, 1974).

Typical values for  $k$  are 2.3 pC/N for quartz and 140 pC/N for barium titanate. For a piezoelectric sensor of 1 cm<sup>2</sup> area and 1 mm thickness with an applied force due to a 10 g weight, the output voltage  $v$  is 0.23 mV and 14 mV for the quartz and barium titanate crystals, respectively.

There are various modes of operation of piezoelectric sensors, depending on the material and the crystallographic orientation of the plate (Lion, 1959). These modes include the thickness or longitudinal compression, transversal compression, thickness-shear action, and face-shear action.

Also available are piezoelectric polymeric films, such as polyvinylidene fluoride (PVDF) (Hennig, 1988; Webster, 1988). These films are very thin, lightweight and pliant, and they can be cut easily and adapted to uneven surfaces. The low mechanical quality factor does not permit resonance applications, but it permits acoustical broadband applications for microphones and loudspeakers.

Piezoelectric materials have a high but finite resistance. As a consequence, if a static deflection  $x$  is applied, the charge leaks through the leakage resistor (on the order of 100 GΩ). It is obviously quite important that the input impedance of the external voltage-measuring device be an order of magnitude higher than that of the piezoelectric sensor. It would be helpful to look at the

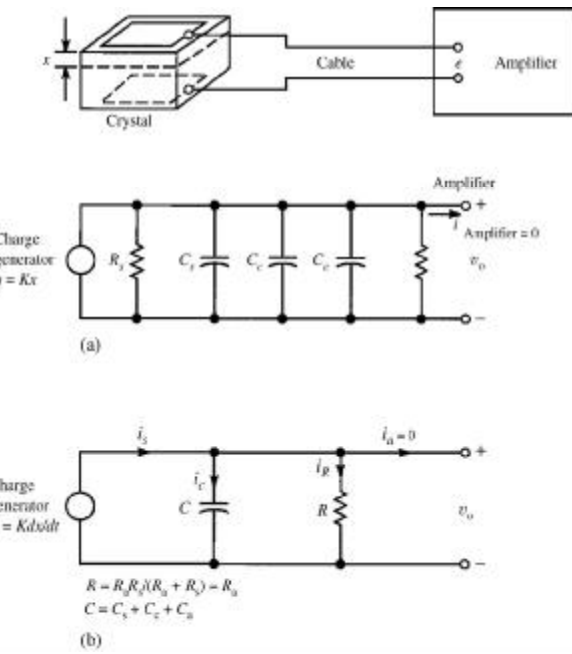


**Figure 2.10** (a) Equivalent circuit of piezoelectric sensor, where  $R_s$  = sensor leakage resistance,  $C_s$  = sensor capacitance,  $C_c$  = cable capacitance,  $C_a$  = amplifier input capacitance,  $R_a$  = amplifier input resistance, and  $q$  = charge generator. (b) Modified equivalent circuit with current generator replacing charge generator. (From *Measurement Systems: Application and Design*, by E. O. Doebelin. Copyright © 1990 by McGraw-Hill, Inc. Used with permission of McGraw-Hill Book Co.)

equivalent circuit for the piezoelectric sensor [Figure 2.10(a)] in order to quantify its dynamic-response characteristics.

This circuit has a charge generator  $q$  defined by

$$q = Kx \quad (2.15)$$

where where

$K$  = proportionality constant, C/m

$x$  = deflection

The circuit may be simplified by converting the charge generator to a current generator,  $i_s$ .

$$i_s = \frac{dq}{dt} = K \frac{dx}{dt} \quad (2.16)$$

The modified circuit is shown in Figure 2.10(b), where the resistances and capacitances have been combined. Assuming that the amplifier does not draw any current, we then have

$$i_s = i_C + i_R \quad (2.17)$$

$$v_o = v_C = \left(\frac{1}{C}\right) \int i_C dt \quad (2.18)$$

$$i_s - i_R = C \left(\frac{dv_o}{dt}\right) = K \frac{dx}{dt} - \frac{v_o}{R} \quad (2.19)$$

or

$$\frac{V_o(j\omega)}{X(j\omega)} = \frac{K_s j\omega \tau}{j\omega \tau + 1} \quad (2.20)$$

where

$$K_s = K/C \text{ (sensitivity, V/m)}$$

$$\tau = RC \text{ (time constant)}$$

**EXAMPLE 2.2** A piezoelectric sensor has  $C = 500 \text{ pF}$ . The sensor leakage resistance is  $10 \text{ G}\Omega$ . The amplifier input impedance is  $5 \text{ M}\Omega$ . What is the low-corner frequency?

**ANSWER** We may use the modified equivalent circuit of the piezoelectric sensor given in Figure 2.10(b) for this calculation.

$$f_c = 1/(2\pi RC) = 1/[2\pi(5 \times 10^6)(500 \times 10^{-12} \text{ F} \times 10 \text{ G}\Omega)] = 64 \text{ Hz}$$

Note that by increasing the input impedance of the amplifier by a factor of 100, we can lower the low-corner frequency to 0.64 Hz.

**EXAMPLE 2.3** For a piezoelectric sensor plus cable that has  $1 \text{ nF}$  capacitance, design a *voltage amplifier* (not a charge amplifier) by using only *one* noninverting amplifier that has a gain of 10. It should handle a charge of  $1 \mu\text{C}$  generated by the carotid pulse without saturation. It should not drift into saturation because of bias currents. It should have a frequency response from 0.05 to 100 Hz. Add the minimal number of extra components to achieve the design specifications.

**ANSWER** Calculate the voltage from  $V = Q/C = 1 \mu\text{C}/1 \text{ nF} = 1 \text{ kV}$ . Because this is too high, add a shunt capacitor  $C_s = 1 \mu\text{F}$  to achieve 1.0 V. Allow for a gain of 10. To achieve low-corner frequency, add shunt

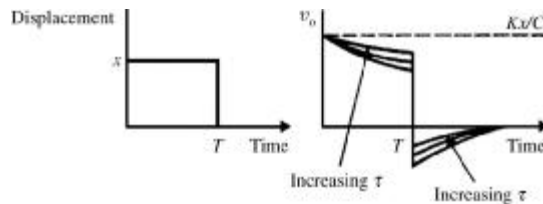


**Figure 2.11** Sensor response to a step displacement (From Doebelin, E. O. 1990. *Measurement Systems: Application and Design*, New York: McGraw-Hill.)

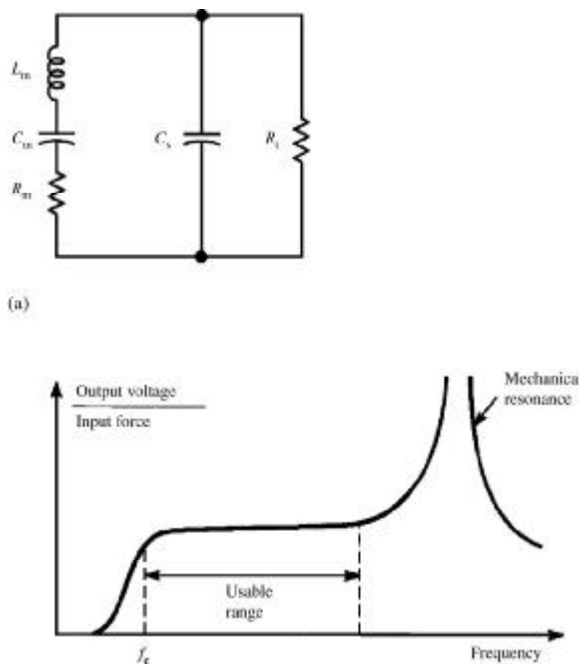
$R_s = 1/2\pi f_c C = 1/2\pi(0.05)(1\ \mu\text{F}) = 3.2\ \text{M}\Omega$ . To achieve gain of +10 in a noninverting amplifier, select  $R_f = 10\ \text{k}\Omega$  and  $R_i = 11.1\ \text{k}\Omega$ . To achieve high-corner frequency,  $C_f = 1/2\pi f_c R_f = 1/2\pi(100)(10\ \text{k}\Omega) = 160\ \text{nF}$ .

Figure 2.11 shows the voltage-output response of a piezoelectric sensor to a step displacement  $x$ . The output decays exponentially because of the finite internal resistance of the piezoelectric material. At time equal to  $T$  the force is released, and a displacement restoration results that is equal to and opposite of the original displacement. This causes a sudden decrease in voltage of magnitude  $Kx/C$ , with a resulting undershoot equal to the decay prior to the release of the displacement. The decay and undershoot can be minimized by increasing the time constant,  $\tau = RC$ . The simplest approach to increasing  $\tau$  is to add a parallel capacitor. However, doing so reduces the sensitivity in the midband frequencies according to (2.20).

Another approach to improving the low-frequency response is to use the charge amplifier described in Section 3.8.

Because of its mechanical resonance, the high-frequency equivalent circuit for a piezoelectric sensor is complex. This effect can be represented by adding a series  $RLC$  circuit in parallel with the sensor capacitance and leakage resistance. Figure 2.12 shows the high-frequency equivalent circuit and its frequency response. Note that in some applications—for example, in the case of crystal filters—the mechanical resonance is useful for accurate frequency control.

Piezoelectric sensors are used quite extensively in cardiology for external (body-surface) and internal (intracardiac) phonocardiography. They are also used in the detection of Korotkoff sounds in blood-pressure measurements (Chapter 7). Additional applications of piezoelectric sensors involve their use in measurements of physiological accelerations. A piezoelectric sensor and circuit can measure the acceleration due to human movements and provide an estimate of energy expenditure (Servais *et al.*, 1984). Section 8.4 describes ultrasonic blood-flow meters in which the piezoelectric element operating at mechanical resonance emits and senses high-frequency sounds. Li and Su (2006) describe piezoelectric sensors as sensitive mass sensors to detect and measure a broad variety of biomedical analytes in both gas and liquid phases based on the adsorption and/or desorption of target analyte(s) on the sensor surface.



**Figure 2.12** (a) High-frequency circuit model for piezoelectric sensor.  $R_s$  is the sensor leakage resistance and  $C_s$  is the capacitance.  $L_m$ ,  $C_m$ , and  $R_m$  represent the mechanical system, (b) Piezoelectric sensor frequency response. (From *Transducers for Biomedical Measurements: Principles and Applications*, by R. S. C. Cobbold. Copyright (c) 1974, John Wiley and Sons, Inc. Reprinted by permission of John Wiley and Sons, Inc.)

## 2.7 TEMPERATURE MEASUREMENTS

A patient's body temperature gives the physician important information about the physiological state of the individual. External body temperature is one of many parameters used to evaluate patients in shock, because the reduced blood pressure of a person in circulatory shock results in low blood flow to the periphery. A drop in the big-toe temperature is a good early clinical warning of shock. Infections, on the other hand, are usually reflected by an increase in body temperature, with a hot, flushed skin and loss of fluids. Increased ventilation, perspiration, and blood flow to the skin result when high fevers destroy temperature-sensitive enzymes and proteins. Anesthesia decreases body temperature by depressing the thermal regulatory center. In fact, physicians routinely induce hypothermia in surgical cases in which they wish to decrease a patient's metabolic processes and blood circulation.

In pediatrics, special heated incubators are used for stabilizing the body temperature of infants. Accurate monitoring of temperature and regulatory

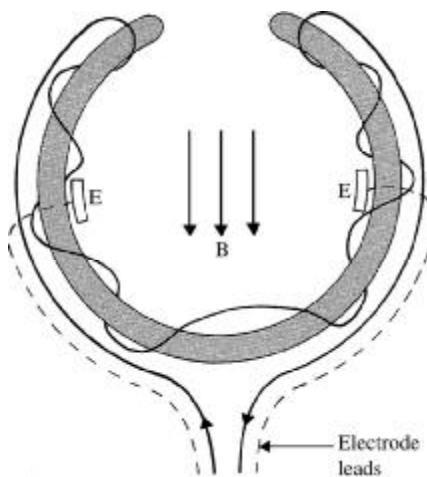


**Figure 8.7** The toroidal-type cuff probe has two oppositely wound windings on each half of the core. The magnetic flux thus leaves the top of both sides, flows down in the center of the cuff, enters the base of the toroid, and flows up through both sides.

resulting magnetic field has low leakage flux. To prevent capacitive coupling between the coils of the magnet and the electrodes, an electrostatic shield is placed between them. The probe is insulated with a potting material that has a very high resistivity and impermeability to salt water (blood is similar to saline).

The open slot on one side of the probe makes it possible to slip it over a blood vessel without cutting the vessel. A plastic key may be inserted into the slot so that the probe encircles the vessel. The probe must fit snugly during diastole so that the electrodes make good contact. This requires some constriction of an artery during systole, when the diameter of the artery is about 7% greater. Probes are made in 1 mm increments in the range of 1 to 24 mm to ensure a snug fit on a variety of sizes of arteries. To be able to measure any size of artery requires a considerable expenditure for probes: Individual probes typically cost \$500 each. The probes do not operate satisfactorily on veins, because the electrodes do not make good contact when the vein collapses. Special flow-through probes are used outside the body for measuring the output of cardiac-bypass pumps.

#### 8.4 ULTRASONIC FLOWMETERS

The ultrasonic flowmeter, like the electromagnetic flowmeter, can measure instantaneous flow of blood. The ultrasound can be beamed through the skin, thus making transcutaneous flowmeters practical. Advanced types of ultrasonic flowmeters can also measure flow profiles. These advantages are making

the ultrasonic flowmeter the subject of intensive development. Let us examine some aspects of this development.

### TRANSDUCERS

For the transducer to be used in an ultrasonic flowmeter, we select a piezoelectric material (Section 2.6) that converts power from electric to acoustic form (Christensen, 1988). Lead zirconate titanate is a crystal that has the highest conversion efficiency. It can be molded into any shape by melting. As it is cooled through the Curie temperature, it is placed in a strong electric field to polarize the material. It is usually formed into disks that are coated on opposite faces with metal electrodes and driven by an electronic oscillator. The resulting electric field in the crystal causes mechanical constriction. The pistonlike movements generate longitudinal plane waves, which propagate into the tissue. For maximal efficiency, the crystal is one-half wavelength thick. Any cavities between the crystal and the tissue must be filled with a fluid or watery gel in order to prevent the high reflective losses associated with liquid–gas interfaces.

Because the transducer has a finite diameter, it will produce diffraction patterns, just as an aperture does in optics. Figure 8.8 shows the outline of the beam patterns for several transducer diameters and frequencies. In the *near field*, the beam is largely contained within a cylindrical outline and there is little spreading. The intensity is not uniform, however: There are multiple maxima and minima within this region, caused by interference. The near field extends a distance  $d_{\text{nf}}$  given by

$$d_{\text{nf}} = \frac{D^2}{4\lambda} \quad (8.9)$$

where  $D$  = transducer diameter and  $\lambda$  = wavelength.

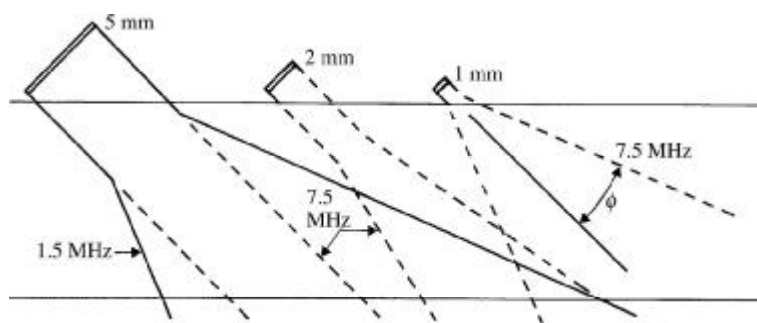


**Figure 8.8** Near and far fields for various transducer diameters and frequencies. Beams are drawn to scale, passing through a 10 mm-diameter vessel. Transducer diameters are 5, 2, and 1 mm. Solid lines are for 1.5 MHz, dashed lines for 7.5 MHz.

In the *far field* the beam diverges, and the intensity is inversely proportional to the square of the distance from the transducer. The angle of beam divergence  $\phi$ , shown in Figure 8.8, is given by

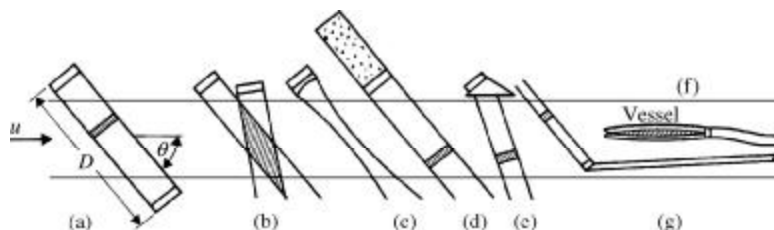
$$\sin \phi = \frac{1.2\lambda}{D} \quad (8.10)$$

Figure 8.8 indicates that we should avoid the far field because of its lower spatial resolution. To achieve near-field operation, we must use higher frequencies and larger transducers.

To select the operating frequency, we must consider several factors. For a beam of constant cross section, the power decays exponentially because of absorption of heat in the tissue. The absorption coefficient is approximately proportional to frequency, so this suggests a low operating frequency. However, most ultrasonic flowmeters depend on the power scattered back from moving red blood cells. The backscattered power is proportional to  $f^4$ , which suggests a high operating frequency. The usual compromise dictates a frequency between 2 and 10 MHz.

### TRANSIT-TIME FLOWMETER

Figure 8.9(a) shows the transducer arrangement used in the transit-time ultrasonic flowmeter (Christensen, 1988). The effective velocity of sound in the vessel is equal to the velocity of sound,  $c$ , plus a component due to  $\hat{u}$ , the



**Figure 8.9 Ultrasonic transducer configurations** (a) A transit-time probe requires two transducers facing each other along a path of length  $D$  inclined from the vessel axis at an angle  $\phi$ . The hatched region represents a single acoustic pulse traveling between the two transducers. (b) In a transcutaneous probe, both transducers are placed on the same side of the vessel, so the probe can be placed on the skin. Beam intersection is shown hatched. (c) Any transducer may contain a plastic lens that focuses and narrows the beam. (d) For pulsed operation, the transducer is loaded by backing it with a mixture of tungsten powder in epoxy. This increases losses and lowers  $Q$ . Shaded region is shown for a single time of range gating. (e) A shaped piece of Lucite on the front loads the transducer and also refracts the beam. (f) A transducer placed on the end of a catheter beams ultrasound down the vessel. (g) For pulsed operation, the transducer is placed at an angle.

velocity of flow of blood averaged along the path of the ultrasound. For laminar flow,  $\hat{u} = 1.33 \bar{u}$ , and for turbulent flow,  $\hat{u} = 1.07 \bar{u}$ , where  $\bar{u}$  is the velocity of the flow of blood averaged over the cross-sectional area. Because the ultrasonic path is along a single line rather than averaged over the cross-sectional area,  $\hat{u}$  differs from  $\bar{u}$ . The transit time in the downstream (+) and upstream (-) directions is

$$t = \frac{\text{distance}}{\text{conduction velocity}} = \frac{D}{c \pm \hat{u} \cos \theta} \quad (8.11)$$

The difference between upstream and downstream transit times is

$$\Delta t = \frac{2 D \hat{u} \cos \theta}{(c^2 - \hat{u}^2 \cos^2 \theta)} \cong \frac{2 D \hat{u} \cos \theta}{c^2} \quad (8.12)$$

and thus the average velocity  $\hat{u}$  is proportional to  $\Delta t$ . A short acoustic pulse is transmitted alternately in the upstream and downstream directions. Unfortunately, the resulting  $\Delta t$  is in the nanosecond range, and complex electronics are required to achieve adequate stability. Like the electromagnetic flowmeter, the transit-time flowmeter and similar flowmeters using a phase-shift principle can operate with either saline or blood as a fluid, because they do not require particulate matter for scattering. However, they do require invasive surgery to expose the vessel.

### CONTINUOUS-WAVE DOPPLER FLOWMETER

When a target recedes from a fixed source that transmits sound, the frequency of the received sound is lowered because of the Doppler effect. For small changes, the fractional change in frequency equals the fractional change in velocity.

$$\frac{f_d}{f_0} = \frac{u}{c} \quad (8.13)$$

where

$f_d$  = Doppler frequency shift

$f_0$  = source frequency

$u$  = target velocity

$c$  = velocity of sound

The flowmeter shown in Figure 8.10 requires particulate matter such as blood cells to form reflecting targets. The frequency is lowered twice. One shift occurs between the transmitting source and the moving cell that receives the

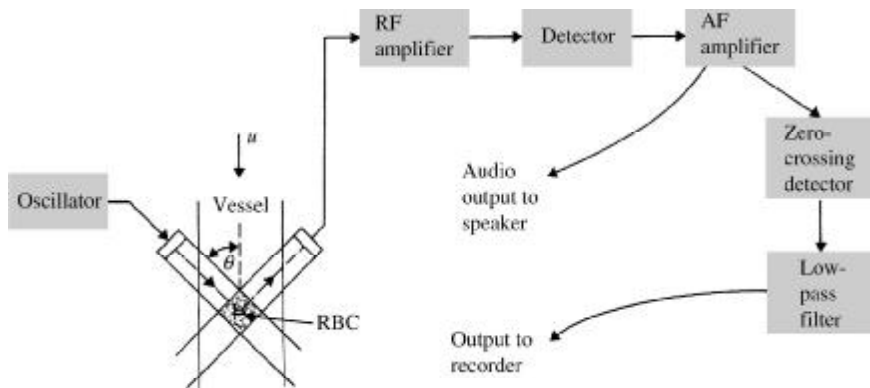


**Figure 8.10** Doppler ultrasonic blood flowmeter In the simplest instrument, ultrasound is beamed through the vessel walls, backscattered by the red blood cells, and received by a piezoelectric crystal.

signal. The other shift occurs between the transmitting cell and the receiving transducer.

$$\frac{f_d}{f_0} = \frac{2u}{c+u} \cong \frac{2u}{c} \quad (8.14)$$

The approximation is valid, because  $c \cong 1500 \text{ m/s}$  and  $u \cong 1.5 \text{ m/s}$ . The velocities do not all act along the same straight line, so we add an angle factor

$$f_d = \frac{2 f_0 u \cos \theta}{c} \quad (8.15)$$

where  $\theta$  is the angle between the beam of sound and the axis of the blood vessel, as shown in Figure 8.10. If the flow is not axial, or the transducers do not lie at the same angle, such as in Figure 8.9(b), we must include additional trigonometric factors.

Figure 8.10 shows the block diagram of a simple continuous-wave flowmeter. The oscillator must have a low output impedance to drive the low-impedance crystal. Although at most frequencies the crystal transducer has a high impedance, it is operated at mechanical resonance, where the impedance drops to about  $100 \Omega$ . The ultrasonic waves are transmitted to the moving cells, which reflect the Doppler-shifted waves to the receiving transducer. The receiving transducer is identical to the transmitting transducer. The amplified radio-frequency (RF) signal plus carrier signal is detected to produce an audio-frequency (AF) signal at a frequency given by (8.15).

Listening to the audio output using a speaker, we get much useful qualitative information. A simple *frequency-to-voltage converter* provides a

quantitative output to a recorder. The *zero-crossing detector* emits a fixed-area pulse each time the audio signal crosses the zero axis. These pulses are low-pass-filtered to produce an output proportional to the velocity of the blood cells.

Although the electromagnetic blood flowmeter is capable of measuring both forward and reverse flow, the simple ultrasonic-type flowmeter full-wave rectifies the output, and the sense of direction of flow is lost. This results because—for either an increase or a decrease in the Doppler-shifted frequency—the beat frequency is the same. Examination of the field intersections shown in Figure 8.10 suggests that the only received frequency is the Doppler-shifted one. However, the received carrier signal is very much larger than the desired Doppler-shifted signal. Some of the RF carrier is coupled to the receiver by the electric field from the transmitter. Because of side lobes in the transducer apertures, some of the carrier signal travels a direct acoustic path to the receiver. Other power at the carrier frequency reaches the receiver after one or more reflections from fixed interfaces. The resulting received signal is composed of a large-amplitude signal at the carrier frequency plus the very low (approximately 0.1%) amplitude Doppler-shifted signal.

The Doppler-shifted signal is not at a single frequency, as implied by (8.15), for several reasons.

1. Velocity profiles are rarely blunt, with all cells moving at the same velocity. Rather, cells move at different velocities, producing different shifts of the Doppler frequency.
2. A given cell remains within the beam-intersection volume for a short time. Thus the signal received from one cell is a pure frequency multiplied by some time-gate function, yielding a band of frequencies.
3. Acoustic energy traveling within the main beam, but at angles to the beam axis, plus energy in the side lobes, causes different Doppler-frequency shifts due to an effective change in  $\theta$ .
4. Tumbling of cells and local velocities resulting from turbulence cause different Doppler-frequency shifts.

All these factors combine to produce a band of frequencies. The resulting spectrum is similar to band-limited random noise, and from this we must extract flow information.

We would like to have high gain in the RF amplifier in order to boost the low-amplitude Doppler-frequency components. But the carrier is large, so the gain cannot be too high or saturation will occur. The RF bandwidth need not be wide, because the frequency deviation is only about 0.001 of the carrier frequency. However, RF-amplifier bandwidths are sometimes much wider than required, to permit tuning to different transducers.

The detector can be a simple square-law device such as a diode. The output spectrum contains the desired difference (beat) frequencies, which lie in the audio range, plus other undesired frequencies.

**EXAMPLE 8.4** Calculate the maximal audio frequency of a Doppler ultrasonic blood flowmeter that has a carrier frequency of 7 MHz, a transducer angle of  $45^\circ$ , a blood velocity of 150 cm/s, and an acoustic velocity of 1500 m/s.

**ANSWER** Substitute these data into (8.15).

$$f_d = \frac{2(7 \times 10^6 \text{ Hz})(1.5 \text{ m/s}) \cos 45^\circ}{1500 \text{ m/s}} \cong 10 \text{ kHz} \quad (8.16)$$

The dc component must be removed with a high-pass filter in the AF amplifier. We require a corner frequency of about 100 Hz in order to reject large Doppler signals due to motion of vessel walls. Unfortunately, this high-pass filter also keeps us from measuring slow cell velocities (less than 1.5 cm/s), such as occur near the vessel wall. A low-pass filter removes high frequencies and also noise. The corner frequency is at about 15 kHz, which includes all frequencies that could result from cell motion, plus an allowance for spectral spreading.

In the simplest instruments, the AF output drives a power amplifier and speaker or earphones. The output is a band of frequencies, so it has a whooshing sound that for steady flows sounds like random noise. Venous flow sounds like a low-frequency rumble and may be modulated when the subject breathes. Arterial flow, being pulsatile, rises to a high pitch once each beat and may be followed by one or more smaller, easily heard waves caused by the under-damped flow characteristics of arteries. Thus this simple instrument can be used to trace and qualitatively evaluate blood vessels within 1 cm of the skin in locations in the legs, arms, and neck. We can also plot the spectrum of the AF signal versus time to obtain a more quantitative indication of velocities in the vessel.

The function of the *zero-crossing detector* is to convert the AF input frequency to a proportional analog output signal. It does this by emitting a constant-area pulse for each crossing of the zero axis. The detector contains a comparator (a Schmitt trigger), so we must determine the amount of hysteresis for the comparator. If the input were a single sine wave, the *signal-to-hysteresis ratio* (SHR) could be varied over wide limits, and the output would indicate the correct value. But the input is band-limited random noise. If the SHR is low, many zero crossings are missed. As the SHR increases, the indicated frequency of the output increases. A SHR of 7 is a good choice because the output does not vary significantly with changes in SHR. Automatic gain control can be used to maintain this ratio. Very high SHRs are not desirable; noise may trigger the comparator. The signal increases and decreases with time because of the beating of the signal components at the various frequencies. Thus the short-term SHR fluctuates, and for a small portion of the time the signal is too low to exceed the hysteresis band.

**EXAMPLE 8.5** Design a comparator with a SHR of 7, as required for the Doppler zero-crossing detector.

**ANSWER** Assume that the signal has been amplified so that its input p-p value equals the  $\pm 10$  V linear range for an op amp. Then our thresholds should be  $\pm 10/7 = \pm 1.4$  V. Use the circuit shown in Figure 3.6(a). Because the input is symmetric about zero,  $v_{ref} = 0$  V. Assume the op amp output saturates at  $\pm 12$  V. The p-p width of the hysteresis loop is four times the voltage across  $R_3$ , or  $2.8/4 = 0.7$ . Assume  $R_3 = 1\text{ k}\Omega$ . Then

$$\frac{R_2 + R_3}{R_3} = \frac{R_2 + 1\text{ k}\Omega}{1\text{ k}\Omega} = \frac{12}{0.7}$$

$R_2 = 16.1\text{ k}\Omega$ . Choose  $R_1 = 10\text{ k}\Omega$ .

The output of the zero-crossing detector is a series of pulses. These pulses are passed through a low-pass filter to remove as many of the high-frequency components as possible. The filter must pass frequencies from 0 to 25 Hz in order to reproduce the frequencies of interest in the flow pulse. However, the signal is similar to band-limited random noise. Thus the pulses are not at uniform intervals, even for a fixed flow velocity, but are more like a Poisson process. Hence the output contains objectionable noise. The low-pass filter must therefore be chosen as a compromise between the high corner frequency desired to reproduce the flow pulse and the low corner frequency desired for good filtering of noise.

A major defect of the detector used in simple flowmeters is that it cannot detect the direction of flow. The recorded output looks as it would if the true velocity had been full-wave rectified. Compared with the electromagnetic flowmeter, this is a real disadvantage, because reverse flow occurs frequently in the body. A first thought might be to translate the Doppler-shifted frequencies not to the region about dc, but to the region about 20 kHz. Forward flow might thus be 30 kHz, and reverse flow 10 kHz. The difficulty with this approach is that the high-amplitude carrier signal is translated to 20 kHz. The Doppler signals are so small that considerable effort is required to build any reasonable frequency-to-voltage converter that is not dominated by the 20 kHz signal.

A better approach is to borrow a technique from radar technology, which is used to determine not only the speed at which an aircraft is flying but also its direction. This is the *quadrature-phase detector*.

Figure 8.11(a) shows the analog portion of the quadrature-phase detector (McLeon, 1967). A phase-shift network splits the carrier into two components that are in quadrature, which means that they are  $90^\circ$  apart. These reference cosine and sine waves must be several times larger than the RF-amplifier output, as shown in Figure 8.12(a). The reference waves and the RF-amplifier output are linearly summed to produce the RF envelope shown in Figure 8.12(b). We assume temporarily that the RF-amplifier output contains no carrier.

If the flow of blood is in the same direction as the ultrasonic beam, we consider the blood to be flowing away from the transducer, as shown in Figure 8.11(a). For this direction, the Doppler-shift frequency is lower than that of the carrier. The phase of the Doppler wave lags behind that of the reference

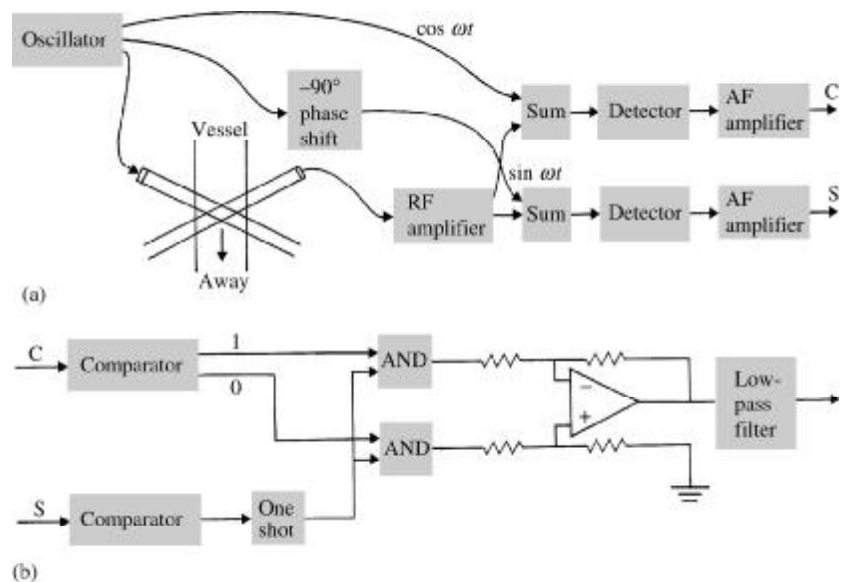


**Figure 8.11** Directional Doppler block diagram (a) Quadrature-phase detector: Sine and cosine signals at the carrier frequency are summed with the RF output before detection. The output C from the cosine channel then leads (or lags) the output S from the sine channel if the flow is away from (or toward) the transducer. (b) Logic circuits route one-shot pulses through the top (or bottom) AND gate when the flow is away from (or toward) the transducer. The differential amplifier provides bidirectional output pulses that are then filtered.

carrier, and the Doppler vector [see Figure 8.12(a)] rotates clockwise. In Figure 8.12(b), for time 1, the carrier and the Doppler add, producing a larger sum in the cosine channel. The sine channel is unchanged. For time 2, the carrier and the Doppler add, producing a larger sum in the sine channel. Similar reasoning produces the rest of the wave for times 3 and 4. Note that the sine channel lags behind the cosine channel.

If the flow of blood is toward the transducer, the Doppler frequency is higher than the carrier frequency, and the Doppler vector rotates counter-clockwise. This produces the dashed waves shown in Figure 8.12(b), and the phase relation between the cosine and sine channels is reversed. Thus, by examining the sign of the phase, we measure direction of flow. The detector produces AF waves that have the same shape as the RF envelope.

Figure 8.11(b) shows the logic that detects the sign of the phase. The cosine channel drives a comparator, the digital output of which, shown in Figure 8.12(b), is used for gating and does not change with direction of flow of blood. The sine channel triggers a one-shot the width of which must be short. Depending on the direction of flow, this one-shot is triggered either at the beginning of or halfway through the period, as shown in Figure 8.12(b). The

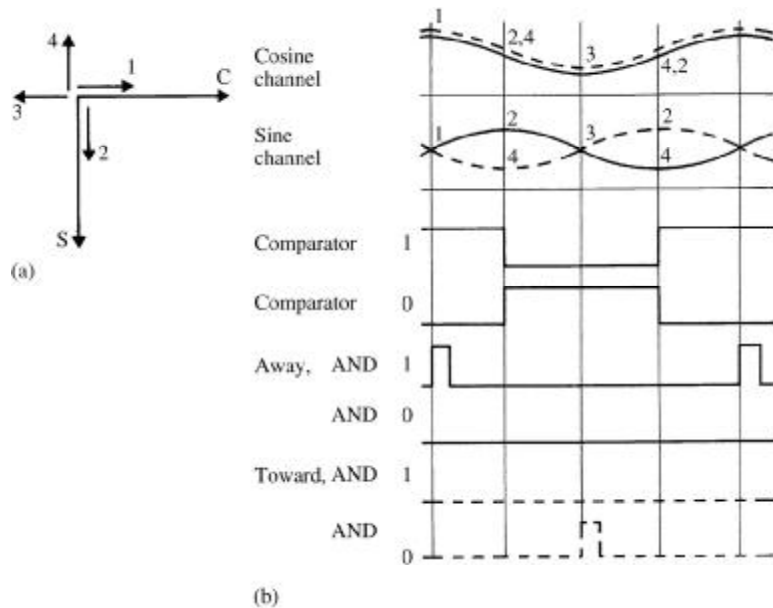


**Figure 8.12** Directional Doppler signal waveforms (a) Vector diagram: The sine wave at the carrier frequency lags the cosine wave by  $90^\circ$ . If flow is away from the transducer, the Doppler frequency is lower than the carrier. The short vector represents the Doppler signal and rotates clockwise, as shown by the numbers 1, 2, 3, and 4. (b) Timing diagram: The top two waves represent the single-peak envelope of the carrier plus the Doppler before detection. Comparator outputs respond to the cosine channel audio signal after detection. One-shot pulses are derived from the sine channel and are gated through the correct AND gate by comparator outputs. The dashed lines indicate flow toward the transducer.

AND gates then gate it into the top or bottom input of the differential amplifier, thus producing a bidirectional output.

The preceding discussion is correct for a sinusoidal RF signal. Our RF signal is like band-limited random noise, however, so there is some time shifting of the relations shown in Figure 8.12(b). Also, a large fixed component at the carrier frequency is present, which displaces the Doppler vectors away from the position shown. As long as the reference cosine and sine waves are more than twice the amplitude of the total RF output, time shifting of the gating relations is not excessive. These time shifts are not problems in practice; a short one-shot pulse can shift almost  $\pm 90^\circ$  before passing out of the correct comparator gate.

It is possible to add another one-shot and several logic blocks to obtain pulse outputs on both positive and negative zero crossings. This doubles the frequency of the pulse train and reduces the fluctuations in the output to 0.707 of their former value.

## PULSED DOPPLER

Continuous-wave flowmeters provide little information about flow profile. Therefore, several instruments have been built (Christensen, 1988) that operate in a radarlike mode. The transmitter is excited with a brief burst of signal. The transmitted wave travels in a single packet, and the transmitter can also be used as a receiver, because reflections are received at a later time. The delay between transmission and reception is a direct indication of distance, so we can obtain a complete plot of reflections across the blood vessel. By examining the Doppler shift at various delays, we can obtain a velocity profile across the vessel.

To achieve good range resolution, the transmitted-pulse duration should ideally be very short. To achieve a good SNR and good velocity discrimination, it should be long. The usual compromise is an 8 MHz pulse of 1  $\mu$ s duration, which produces a traveling packet 1.5 mm long, as shown in Figure 8.9(d). The intensity of this packet is convolved with the local velocity profile to produce the received signal. Thus, the velocity profile of the blood vessel is smeared to a larger-than-actual value. Because of this problem, and also because the wave packet arrives at an angle to normal, the location of the vessel walls is indistinct. It is possible, however, to mathematically “deconvolve” the instrument output to obtain a less smeared representation of the velocity profile.

There are two constraints on pulse repetition rate  $f_r$ . First, to avoid *range ambiguities*, we must analyze the return from one pulse before sending out the next. Thus

$$f_r < \frac{c}{2R_m} \quad (8.17)$$

where  $R_m$  is the maximal useful range. Second, we must satisfy the *sampling theorem*, which requires that

$$f_r > 2f_d \quad (8.18)$$

Combining (8.17) and (8.18) with (8.15) yields

$$u_m(\cos \theta)R_{\max} < \frac{c^2}{8f_0} \quad (8.19)$$

which shows that the product of the range and the maximal velocity along the transducer axis is limited. In practice, measurements are constrained even more than indicated by (8.19) because of (1) spectral spreading, which produces some frequencies higher than those expected, and (2) imperfect cutoff characteristics of the low-pass filters used to prevent *aliasing* (generation of fictitious frequencies by the sampling process).

Because we cannot easily start and stop an oscillator in 1  $\mu$ s, the first stage of the oscillator operates continuously. The transmitter and the receiver both

use a common piezoelectric transducer, so a *gate* is required to turn off the signal from the transmitter during reception. A one-stage gate is not sufficient to isolate the large transmitter signals from the very small received signals. Therefore, two gates in series are used to turn off the transmitter.

The optimal transmitted signal is a pulse-modulated sine-wave carrier. Although it is easy to generate this burst electrically, it is difficult to transduce this electric burst to a similar acoustic burst. The crystal transducer has a high  $Q$  (narrow bandwidth) and therefore rings at its resonant frequency long after the electric signal stops. Therefore, the transducer is modified to achieve a lower  $Q$  (wider bandwidth) by adding mass to the back [Figure 8.9(d)] or to the front [Figure 8.9(e)]. The  $Q$  is not lowered to a desirable value of about 2 to 5, because this would greatly decrease both the efficiency of the transmission and the sensitivity of the reception. The  $Q$  is generally 5 to 15, so some ringing still exists.

When we generate a short sine-wave burst, we no longer have a single frequency. Rather, the pulse train of the repetition rate is multiplied by the carrier in time, producing carrier sidebands in the frequency domain. This spectrum excites the transducer, producing a field that is more complex than that for continuous-wave excitation. This causes spectral spreading of the received signal.

### LASER DOPPLER BLOOD FLOWMETER

In a laser Doppler blood flowmeter, a 5 mW He-Ne laser beams 632.8 nm light through fiber optics into the skin (Khaodhia and Veves, 2006). Moving red blood cells in the skin frequency shift the light and cause spectral broadening. Reflected light is carried by fiber optics to a photodiode. Filtering, weighting, squaring, and dividing are necessary for signal processing. Capillary blood flow has been studied in the skin and many other organs.

---

## 8.5 THERMAL-CONVECTION VELOCITY SENSORS

---

### PRINCIPLE

The thermodilution methods described in Sections 8.1 and 8.2 depend on the mixing of the heat indicator into the entire flow stream. In contrast, thermal velocity sensors depend on convective cooling of a heated sensor and are therefore sensitive only to local velocity.

Figure 8.13(a) shows a simple probe. The thermistor  $R_u$  is heated to a temperature difference  $\Delta T$  above blood temperature by the power  $W$  dissipated by current passing through  $R_u$ . Experimental observations (Grahn *et al.*, 1969) show that these quantities are related to the blood velocity  $u$  by

$$\frac{W}{\Delta T} = a + b \log u \quad (8.20)$$